INT. J. CONTROL, 2003, VOL. 76, NO. 16, 1635–1643

Taylor & Francis
Taylor & Francis Group

Control of batch cooling crystallization processes based on orbital flatness

ULRICH VOLLMER† and JÖRG RAISCH‡*

In this article it is shown that moment models for batch crystallization processes are orbitally flat. The state dependent time scaling involved in orbital flatness is physically meaningful and leads to a notion of time that is very natural for the crystallization process. A procedure is presented to check if a desired final crystal size distribution (CSD) is achievable and to compute the temporal temperature profile that produces this desired CSD. Furthermore, the problem of dynamic optimization of the crystallizer operation is reformulated based on the system's flatness property such that the differential equations are eliminated from the optimization problem. In a case study the effectiveness of this optimization is demonstrated.

1. Introduction

Crystallization is well established in the chemical and pharmaceutical industry as a purification and separation technique. In batch mode, crystallization is used for the small-scale production of fine chemicals and pharmaceuticals. Commonly, chemical reaction steps take place in liquids—solutions or melts—while final products often are solids. In many of these cases, the solid product is obtained by crystallization.

The quality of such crystalline products is determined not only by their chemical composition but also by physical properties, such as crystal size distribution (CSD) and morphology of crystals. The production of crystalline material with a pre-defined size distribution is one of the major challenges in industrial crystallization (Rawlings *et al*. 1993). In batch cooling crystallizers, the fact that solubility depends on temperature is exploited. The solution (material to be crystallized dissolved in some solvent) is cooled such that it becomes supersaturated. In the supersaturated liquid, two main processes take place. New crystals emerge from solution and existing crystals grow. Since both processes, nucleation and growth, are active during the entire batch time, the product obtained at the end of the batch contains crystals of different sizes. As the rates of nucleation and crystal growth depend on the degree of supersaturation and supersaturation, in turn, is a function of temperature, the final product CSD can be influenced by the temperature-time-profile during the batch.

Received 1 December 2002. Revised and accepted 19 September 2003.

*Author for correspondence. e-mail: raisch@mpi-magdeburg.mpg.de

†Systems and Control Theory Group, Max-Planck-Institut Dynamik komplexer technischer Systeme, 39106 Magdeburg, Germany.

‡Systems and Control Theory Group, Max-Planck-Institut Dynamik komplexer technischer Systeme, 39106 Magdeburg, Germany and Lehrstuhl für Systemtheorie technischer Prozesse, Otto-von-Guericke-Universität, 39016 Magdeburg, Germany.

Crystallization processes are adequately described by *population balance models* (Randolph and Larson 1988, Ramkrishna 2000). These are distributed parameter systems typically consisting of a partial differential equation (PDE) describing the evolution of the CSD, which is a function of time and crystal size, coupled with one or more ordinary differential equations (ODE) for concentration and temperature of the liquid phase. Under certain conditions, a finite dimensional model can be derived from the population balance, which does not describe the evolution of the entire CSD, but only of a number of moments of the size distribution.

Based on a population balance model, it is of course possible to determine the final product CSD for a given temperature profile by simulation. The inverse problem, i.e. the design of a feedforward control which produces a desired CSD, is an area of active research. The most common approach is to use optimization techniques in order to determine a temperature profile that minimizes, for example, the coefficient of variation of the CSD or maximizes the mean size of crystals. Jones (1974) applied Pontryagin's maximum principle to obtain an optimal cooling policy. Dynamic optimization was applied, for example, in Miller and Rawlings (1994) and Lang *et al*. (1999). This approach handles path constraints and final time constraints. Chung *et al*. (1999) used the seed crystal distribution as an additional degree of freedom during optimization. Zhang and Rohani (2002) correct the temperature trajectory during the batch by re-running the optimization on-line. Thus, it is possible to react to disturbances. Others argued that keeping the supersaturation constant over the batch run had a positive effect on final CSD. Therefore, Jones and Mullin (1974) designed a temperature trajectory to keep supersaturation constant and Xie *et al*. (2001) designed a non-linear feedback controller to achieve the same objective.

In this contribution, the feedforward control problem for batch cooling crystallizers is addressed using non-linear control methods. The design of *feedback* con-

International Journal of Control ISSN 0020–7179 print/ISSN 1366–5820 online © 2003 Taylor & Francis Ltd
http://www.tandf.co.uk/journals
DOI: 10.1080/00207170310001626419

trollers for non-linear systems has attracted considerable attention. An impressive array of methods has been developed. In contrast, only little work has been devoted to the question of trajectory planning and feedforward control. These problems are usually addressed in an optimization framework. A notable exception is the work on *differential flatness* which was initiated by Fliess *et al.* (1992, 1995 b). The batch crystallizer model can be shown to be differentially flat after an appropriate time scaling. Such systems are called *orbitally flat* (Fliess *et al.* 1995 a, Respondek 1998, Guay 1999). It is well known that flat systems possess a certain invertibility property and, therefore, trajectory planning and feedforward control design can be done in a very elegant way (Rouchon *et al.* 1993). Recently, the flatness concept has been extended to delay systems and to distributed parameter systems (see, e.g. Rudolph and Mounier 2001 and Rudolph 2000).

The article is organized as follows. In § 2, the notion of orbital flatness is defined. In § 3, a population balance model for a batch cooling crystallizer is presented and a finite dimensional moment model for this system is derived. In § 4, using a physically meaningful time scaling, it is shown that the moment model is orbitally flat. Furthermore, a procedure is presented that allows the direct analytic determination of a temperature profile which produces any given final CSD compatible with the model. This is, to the authors' knowledge, the first time this problem has been solved for batch crystallization. Finally, in § 5, a dynamic optimization problem taken from Miller and Rawlings (1994) is treated. Exploiting the system's flatness property, the differential equations can be eliminated from the optimization problem such that the evaluation of the objective function does not involve numerical solution of the system model any more.

2. Orbital flatness

The notion of flatness can be mathematically defined in a differential algebra setting (Fliess *et al.* 1995 b) or in the context of differential geometry of infinite jets and prolongations (Fliess *et al.* 1999). In this section, a less formal, more intuitive definition of flatness is given (Rothfuß *et al.* 1996). A finite dimensional dynamic system

$$\dot{x}(t) = f(x(t), u(t)), \quad x(t) \in \mathbb{R}^n,\ u(t) \in \mathbb{R}^m \tag{1}$$

is called *differentially flat*, or simply *flat*, if there exists a fictitious output $y(t) \in \mathbb{R}^m$ which satisfies the following conditions.

A The output $y(t)$ can be expressed as a function of the system states $x(t)$ and inputs $u(t)$ and finitely many time derivatives of the inputs

$$y(t) = \Phi(x(t), u(t), \dot{u}(t), \ldots, u^{(\alpha)}(t)) \tag{2}$$

B Reversely, the system states and inputs can be expressed as functions of the output $y(t)$ and finitely many of its time derivatives

$$x(t) = \Psi_1(y(t), \dot{y}(t), \ldots, y(t)^{(\beta)}) \tag{3 a}$$

$$u(t) = \Psi_2(y(t), \dot{y}(t), \ldots, y(t)^{(\beta+1)}) \tag{3 b}$$

The fictitious output $y(t)$ is then called a *flat output*. It completely determines the dynamic behaviour of system (1). If a sufficiently smooth trajectory of the flat output is given, the trajectories of the entire system state $x(t)$ and the system input $u(t)$ are determined by (3 *a*) and (3 *b*), respectively. They can be computed without solving a differential equation. Therefore, it is obvious that flatness is a property which facilitates the problems of trajectory planning and design of feedforward control considerably. Since the flat output constitutes an algebraic parameterization of the system's dynamics, flatness is a particularly useful property for the solution of dynamic optimization problems. Furthermore, flatness is closely related to linearizability of non-linear systems by feedback. For single-input systems, for example, flatness is equivalent to linearizability by static state feedback.

The advantages of flat systems can be extended to a somewhat larger class of systems allowing an appropriate state-dependent time scaling (Fliess *et al.* 1995 a, Respondek 1998, Guay 1999). A new 'time'-variable τ is defined as

$$[t_0 \quad t_{\text{end}}] \mapsto [\tau_0 \quad \tau_{\text{end}}]$$
$$\frac{\mathrm{d}t}{\mathrm{d}\tau} = s(x(t), u(t)), \quad \tau(t_0) = \tau_0 \tag{4}$$

For the mapping of t to τ to be bijective, the scaling function $s(x(t), u(t))$ has to satisfy

$$0 < s(x(t), u(t)) < \infty, \quad \forall t \tag{5}$$

This condition ensures that τ is a monotonically increasing function in t and goes to infinity if and only if t goes to infinity, as intuitively expected from a proper notion of 'time'. Furthermore, equation (5) makes the time transformation invertible such that a control law $u(\tau)$ designed in new time τ can be transformed back and applied in real time t. In new 'time', the system (1) evolves according to

$$\frac{\mathrm{d}x}{\mathrm{d}\tau} = f(x(\tau), u(\tau))s(x(\tau), u(\tau)) =: g(x(\tau), u(\tau)) \tag{6}$$

If the time-scaled system (6) is flat then the original system (1) is called *orbitally flat*.

3. Population balance model for batch crystallizer

A batch cooling crystallizer is depicted in figure 1. It is operated as follows. Initially the vessel is filled with hot undersaturated solution. Then, the crystallizer is cooled such that the liquid becomes supersaturated. At this point, small seed crystals may be added. Due to supersaturation, new crystals are formed and existing crystals grow. Nucleation and growth consume solute from the solution such that the concentration decreases. Hence, further cooling is necessary to keep the liquid supersaturated. To prevent settling of crystals, the slurry is mixed by an impeller. At the end of the batch the vessel is discharged and the crystalline product undergoes further processing steps such as filtering and drying. The quality of the product as well as the efficiency of downstream processing is heavily influenced by the CSD.

For process modelling, the size of crystals is defined by a characteristic length L (e.g. the edge length in the case of cubic crystals). The CSD is described by the number density function $f(L,t)$, which represents the number of crystals per crystal length and volume of slurry. The number of crystals N in the size range $L_0 < L < L_1$ in the crystallizer therefore is

$$N(t) = V \int_{L_0}^{L_1} f(L,t)\,\mathrm{d}L$$

with volume of slurry V. In the following, a batch crystallizer model is presented which is standard in the crystallization literature. The underlying assumptions are that all crystals grow at the same rate, i.e. the growth rate G is independent of crystal size, and that nuclei are formed at negligible size. Furthermore, attrition, breakage and agglomeration of crystals is neglected. Balancing the number of crystals in an infinitesimal interval of crystal length, a PDE is obtained which,

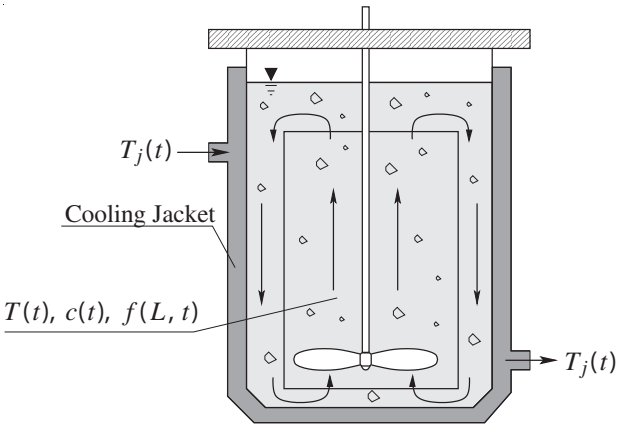

Figure 1. Sketch of a batch cooling crystallizer.

together with appropriate initial and boundary conditions, describes the temporal evolution of the CSD

$$\frac{\partial f(L,t)}{\partial t} = -\frac{\partial (G(t) f(L,t))}{\partial L} \tag{7a}$$

$$f(0,t) = \frac{B(t)}{G(t)} \tag{7b}$$

$$f(L,0) = f_{\mathrm{seed}}(L) \tag{7c}$$

The rate of nucleation is denoted by $B(t)$ and the CSD of seed crystals added at the beginning of the batch is named $f_{\mathrm{seed}}(L)$. Equation (7 *a*) is called the *population balance*. For details of crystallizer modelling see Randolph and Larson (1988). A mole balance for the liquid phase yields an ordinary differential equation for the solute concentration $c(t)$

$$\frac{\mathrm{d}c(t)}{\mathrm{d}t} = -3\rho_c k_v h \int_0^{\infty} L^2 G(t) f(L,t)\,\mathrm{d}L \tag{8}$$

where ρ_c is the density of crystals, h is a conversion factor equal to the volume of slurry per mass of solvent and k_v is a volume shape factor defined such that the volume of a crystal with length L is $V_{\mathrm{crystal}}(L) = k_v L^3$.

Nucleation and growth rates depend on supersaturation $S(t)$ and CSD $f(L,t)$

$$G(t) = k_g S(t)^g \tag{9}$$

$$B(t) = k_b S(t)^b k_v \int_0^{\infty} L^3 f(L,t)\,\mathrm{d}L \tag{10}$$

with supersaturation

$$S(t) = \frac{c(t) - c_{\mathrm{sat}}(t)}{c_{\mathrm{sat}}(t)} \tag{11}$$

The dependence of saturation concentration c_{sat} on temperature T is represented approximately by a second-order expression

$$c_{\mathrm{sat}}(t) = A_0 + A_1 T(t) + A_2 T(t)^2 \tag{12}$$

The growth and nucleation laws (9) and (10) are empirical relations *not* derived directly from first principles. Values for the parameters k_g, k_b, g and b have to be identified from measurements with the specific plant to be modelled. The parameters depend on the material to be crystallized, the crystallizer geometry and operating conditions whereas A_0, A_1 and A_2 are solely determined by the combination of solute and solvent substances.

Thus, crystallizer temperature $T(t)$ determines saturation concentration $c_{\mathrm{sat}}(t)$ and hence it influences the rates of nucleation $B(t)$ and growth $G(t)$ via supersaturation $S(t)$. In the following, crystallizer temperature $T(t)$ is considered to be the manipulated variable, although of course, only the inlet temperature to the cooling jacket $T_j(t)$ can actually be manipulated.

Viewing $T_j(t)$ as the manipulated variable would make it necessary to add an ODE for temperature $T(t)$ derived from an energy balance for the crystallizer. However, it is common practice in batch crystallization control to use a fast feedback controller that manipulates $T_j(t)$ and makes sure that the crystallizer temperature $T(t)$ tracks its desired value such that the temperature $T(t)$ can be pretended to be the manipulated variable. This approach has the advantage that uncertainties in the transfer behaviour from $T_j(t)$ to $T(t)$ are compensated by feedback.

Equations (7 *a*)–(12) constitute an infinite-dimensional model for the batch crystallizer. It basically consists of a PDE (7 *a*) with boundary condition (7 *b*) coupled with an ODE (8). From the PDE with boundary condition, a set of ODEs for the moments of the CSD

$$\mu_i(t) = \int_0^\infty L^i f(L,t)\,\mathrm{d}L, \quad i = 0,1,2,\ldots \tag{13}$$

can be derived. The zeroth moment $\mu_0(t)$ gives the overall number of crystals. The second moment $\mu_2(t)$ is proportional to the overall crystal surface, and the third moment $\mu_3(t)$ is proportional to the volume of the crystalline material in the crystallizer. Since the duration of the batch t_{end} and the growth rate $G(t)$ are finite

$$t_{\mathrm{end}} < \infty \tag{14 a}$$

$$G(t) < \infty, \quad \forall t \tag{14 b}$$

it follows that the size of crystals is bounded. Hence, there is a maximum length L_{max} such that the following is true

$$f(L,t) = 0, \quad \forall L > L_{\max} \tag{15}$$

Consequently, by partial integration it follows from (7 *a*) and (7 *b*) that

$$\left.\begin{aligned} \frac{\mathrm{d}\mu_0(t)}{\mathrm{d}t} &= B(t) \\ \frac{\mathrm{d}\mu_i(t)}{\mathrm{d}t} &= iG(t)\mu_{i-1}(t), \quad i = 1,2,\ldots \end{aligned}\right\} \tag{16}$$

Since the overall mass of solute in the crystallizer, dissolved plus crystalline, is constant an additional algebraic equation can be derived, relating the third moment $\mu_3(t)$ and the solute concentration $c(t)$

$$c(t) = c_0 + \rho_c k_v h(\mu_{3,\mathrm{Seed}} - \mu_3(t)) \tag{17}$$

where c_0 is the initial solute concentration and $\mu_{3,\mathrm{Seed}} := \int_0^\infty f_{\mathrm{seed}}(L)\,\mathrm{d}L$ is the third moment of the seed CSD. Note that the integral expression in (10) is the third moment, i.e. $B(t) = k_b k_v S(t)^b \mu_3(t)$. Because of (9), (11), (12) and (17), $B(t)$ and $G(t)$ are entirely determined by $\mu_3(t)$ and $T(t)$. Hence, the differential equations for the first four moments can be written as

$$\frac{\mathrm{d}\mu_0(t)}{\mathrm{d}t} = B(\mu_3(t), T(t)) \tag{18 a}$$

$$\frac{\mathrm{d}\mu_1(t)}{\mathrm{d}t} = G(\mu_3(t), T(t)) \cdot \mu_0(t) \tag{18 b}$$

$$\frac{\mathrm{d}\mu_2(t)}{\mathrm{d}t} = 2G(\mu_3(t), T(t)) \cdot \mu_1(t) \tag{18 c}$$

$$\frac{\mathrm{d}\mu_3(t)}{\mathrm{d}t} = 3G(\mu_3(t), T(t)) \cdot \mu_2(t) \tag{18 d}$$

This constitutes a simplified model for the batch crystallizer. It is clearly non-linear, but finite-dimensional. The moments $\mu_0(t) \ldots \mu_3(t)$ are the system states, and temperature $T(t)$ is the control input. This model exactly describes the dynamics of the moments of the CSD but it does not, of course, describe the evolution of the entire CSD. However, as will be seen in the following section, both model formulations—population balance model and moment model—play their specific role in the feedforward control design.

4. Control of batch crystallizer

4.1. *Flatness of crystallizer model*

In the following, it is shown that the moment model (18 *a*)–(18 *d*) is orbitally flat. Using the scaling function

$$s(t) = \frac{1}{G(\mu_3(t), T(t))} \tag{19}$$

a new notion of time is introduced by

$$\mathrm{d}\tau = G(\mu_3(t), T(t))\mathrm{d}t, \quad \tau_0 = 0 \tag{20}$$

As G represents the crystal growth rate, the new 'time' τ is the length which a crystal has gained since the beginning of the batch. This is a very natural way to describe the progression of the batch. According to (5) the scaling function has to be strictly positive and finite. For the specific scaling function (19) used here this condition is equivalent to the crystal growth rate $G(\mu_3, T)$ being strictly positive and finite. Because of (9) and (11), this reduces to the requirement that the solution has to be kept supersaturated, i.e. $c(t) > c_{\mathrm{sat}}(t)$, $\forall t$. Since in a crystallizer crystals are to be grown rather than dissolved this condition makes eminent sense from a practical point of view. Using new time τ, the system (18 *a*)–(18 *d*) is transformed to

$$\frac{\mathrm{d}\mu_0(\tau)}{\mathrm{d}\tau} = \frac{B(\mu_3(\tau), T(\tau))}{G(\mu_3(\tau), T(\tau))} \tag{21 a}$$

$$\frac{\mathrm{d}\mu_1(\tau)}{\mathrm{d}\tau} = \mu_0(\tau) \tag{21 b}$$

$$\frac{\mathrm{d}\mu_2(\tau)}{\mathrm{d}\tau} = 2\mu_1(\tau) \tag{21 c}$$

$$\frac{\mathrm{d}\mu_3(\tau)}{\mathrm{d}\tau} = 3\mu_2(\tau) \tag{21 d}$$

It is now shown that for the output

$$y(\tau) = \mu_3(\tau) \tag{22}$$

both conditions A and B in the definition of flatness hold. As $\mu_3(\tau)$ is a state variable, equation (2) and therefore requirement A hold trivially. Differentiating the output $y(\tau)$ four times with respect to τ yields

$$\frac{\mathrm{d}y(\tau)}{\mathrm{d}\tau} = 3\mu_2(\tau) \tag{23 a}$$

$$\frac{\mathrm{d}^2y(\tau)}{\mathrm{d}\tau^2} = 6\mu_1(\tau) \tag{23 b}$$

$$\frac{\mathrm{d}^3y(\tau)}{\mathrm{d}\tau^3} = 6\mu_0(\tau) \tag{23 c}$$

$$\frac{\mathrm{d}^4y(\tau)}{\mathrm{d}\tau^4} = 6\frac{B(\mu_3(\tau), T(\tau))}{G(\mu_3(\tau), T(\tau))} \tag{23 d}$$

From (22), (23 *a*)–(23 *c*) it is immediately clear that the states $\mu_3(\tau) \ldots \mu_0(\tau)$ can be computed from $y(\tau)$ and its first three derivatives. The input $T(\tau)$ can be determined from (23 *d*) by additionally using the fourth derivative. Hence, equations (3 *a*), (3 *b*) and therefore requirement B also hold. Consequently, $y(\tau)$ is a flat output, and the time scaled model (21 *a*)–(21 *d*) is flat, implying that (18 *a*)–(18 *d*) is an orbitally flat system.

4.2. *Feedforward control design*

In the following, two characteristics of the batch crystallizer model are exploited to facilitate feedforward control design. These characteristics are, on the one hand, the orbital flatness property of the moment model and, on the other hand, the simple form of the population balance equation (7 *a*) when rewritten in new time τ. Applying the time transformation (20) to the original PDE (7 *a*) yields the simple transport equation

$$\frac{\partial f(L,\tau)}{\partial \tau} = -\frac{\partial f(L,\tau)}{\partial L} \tag{24}$$

This implies that $f(L,\tau)$ is constant on straight lines in the (L,τ)-domain with $(\mathrm{d}L)/(\mathrm{d}\tau) = 1$, see figure 2. Furthermore, the size distribution $f(L,\tau)$ can be split into two parts, where one part represents grown seed crystals

$$f_s(L,\tau) = f(L,\tau), \quad \text{for } L \geq \tau \tag{25}$$

and the other part describes the distribution of crystals produced by nucleation

$$f_n(L,\tau) = f(L,\tau), \quad \text{for } L < \tau \tag{26}$$

Obviously, the distribution of grown seed crystals $f_s(L,\tau)$ cannot be influenced by control since it is equivalent to the initial seed distribution shifted in size by the length $\Delta L = \tau$: $f_s(L,\tau) = f_{\text{seed}}(L-\tau)$. In contrast, the distribution of particles created by nucleation

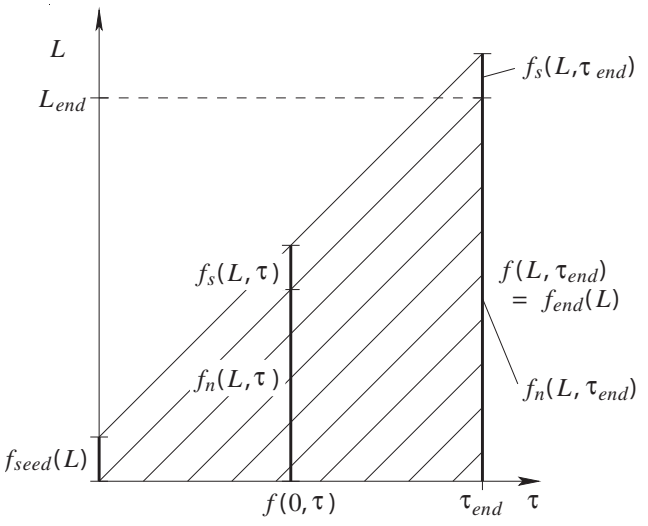

Figure 2. Evolution of CSD in the (L,τ)-domain.

$f_n(L,\tau)$ can be influenced by appropriate manipulation of the crystallizer temperature $T(\tau)$, since the nucleation rate $B(\tau)$ is temperature dependent. Consequently, a necessary condition for a desired CSD at the end of the batch $f_{\text{end}}(L)$ to be attainable is

$$f_{\text{end}}(L) = f_{\text{seed}}(L - \Delta L_{\text{end}}), \text{ for } L \geq \Delta L_{\text{end}} \tag{27}$$

where $\Delta L_{\text{end}} = \tau_{\text{end}}$ is the increase in size which a crystal gains over the whole batch run.

Since $f(L,\tau)$ is constant on the characteristic lines $(\mathrm{d}L)/(\mathrm{d}\tau) = 1$, the values of a desired $f_{\text{end}}(L)$ in the size range $0 \leq L < \Delta L_{\text{end}}$ can be traced back to values of the CSD at the lower boundary of the size range $f(0,\tau)$ for $0 < \tau \leq \tau_{\text{end}}$. Consequently, if the CSD at the end of the batch is fixed to a certain desired distribution

$$f(L,\tau_{\text{end}}) = f_{\text{end}}(L) \tag{28}$$

then the time profile of the boundary condition that is necessary to produce the desired distribution $f_{\text{end}}(L)$ is determined by

$$f(0,\tau) = f_{\text{end}}(\tau_{\text{end}} - \tau), \quad 0 < \tau \leq \tau_{\text{end}} \tag{29}$$

Note that τ_{end} is the maximum length of nucleated crystals, which is also fixed when choosing the desired final CSD $f_{\text{end}}(L)$. Because of (7 *b*) and (23 *d*), this determines the fourth derivative of the flat output

$$\frac{\mathrm{d}^4y(\tau)}{\mathrm{d}\tau^4} = 6f_{\text{end}}(\tau_{\text{end}} - \tau) \tag{30}$$

Integrating this expression four times yields the flat output as a function of new time τ. According to the definition of flatness, all system states and the system input can be determined from the flat output and its derivatives. In particular, this means that a feedforward control $T(\tau)$ can be determined that produces the

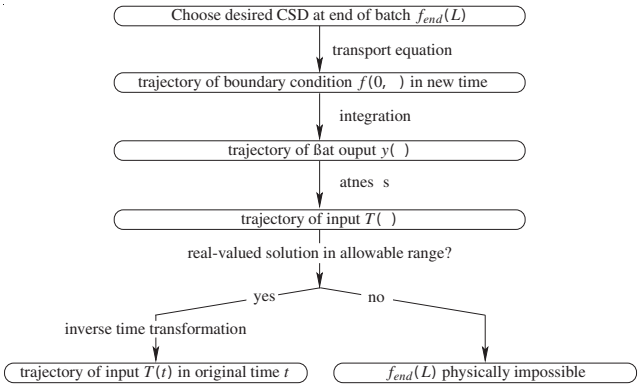

Figure 3. Open loop control design procedure.

desired final CSD $f_{\mathrm{end}}(L)$. Eventually, the time transformation has to be inverted to obtain the control $T(t)$ in original time. The inversion involves integration of (20). This integration cannot be done analytically in general but may have to be done numerically. In these cases, the open loop control $T(t)$ can only be determined at a number of time instances but not as an explicit function of time. However, this is not a severe restriction for practical implementation. Consequently, a procedure is obtained to determine the temperature–time profile producing any desired final CSD. This procedure is summarized schematically in figure 3. Due to the quadratic expression in (12) the procedure yields two solutions for $T(\tau)$ of which at most one is physically meaningful. If both results are not meaningful, for example, in the case of complex conjugate solutions, this implies that the desired CSD $f_{\mathrm{end}}(L)$ is not compatible with the model, i.e. it cannot be produced by the given system from the given initial CSD $f_{\mathrm{seed}}(L)$.

In summary, the flatness property of the crystallizer model can be exploited for the following tasks: checking if a desired final CSD $f_{\mathrm{end}}(L)$ is physically possible and computing the temperature trajectory $T(t)$ which produces a specific $f_{\mathrm{end}}(L)$. Moreover, the flatness property can be exploited for dynamic optimization of the CSD. This will be shown in the next section.

5. Application: minimization of nucleated crystal mass

As pointed out in § 1, a number of researchers have applied dynamic optimization for the design of open loop control strategies for batch crystallizers (see Miller and Rawlings 1994, Chung *et al.* 1999, Lang *et al.* 1999, Zhang and Rohani 2002). Commonly, dynamic optimization based on moment models is used to obtain a temperature trajectory that optimizes a given characteristic of the CSD. Typical objectives are the maximization of the maximum crystal size or the weight mean size of crystals. Since in some situations it is desirable to suppress nucleation as much as possible, another common optimization objective is the minimization of the ratio of the mass of crystals that have been produced by nucleation and the mass of grown seed crystals. Dynamic optimization has also been used on-line in order to be able to react to uncertainties or disturbances.

In Guay *et al.* (2001), it was shown that exploiting the invertibility of (orbitally) flat systems, dynamic optimization problems can be facilitated significantly. As shown in § 2, a flat output completely parameterizes the corresponding dynamic system. If the flat output trajectory is known, the state and input trajectories (and hence any objective function depending on the states) can be determined without solving a differential equation. Therefore, if the flat output is parameterized, e.g. via splines, the complete system is parameterized and the dynamic optimization problem is reduced to a parameter optimization problem.

In the following, we investigate the problem of crystallization of KNO_3 from water in a 3 l crystallizer. We use a model proposed by Miller and Rawlings (1994). This model is of the form of (18 *a*)–(18 *d*) with growth and nucleation functions according to (9) and (10). The parameter values are given in table 1. The initial condition is chosen to be

$$C_0 = 0.493\,\frac{g_{\mathrm{KNO_3}}}{g_{\mathrm{H_2O}}} \tag{31}$$

$$f_{\mathrm{seed}}(L) = \frac{N_{\mathrm{seed}}}{V}\cdot\delta(L - L_{\mathrm{seed}}) \tag{32}$$

where $\delta(\bullet)$ is the Dirac delta impulse. The number of seed crystals N_{seed} is chosen corresponding to an initial mass of seeds of 0.05 g. The size of seed crystals is $L_{\mathrm{seed}} = 196\,\mu\mathrm{m}$.

Based on this model, the following optimization problem is considered. The objective is to minimize the ratio of nucleated crystal mass to final seed crystal mass

Growth coefficient	k_g	6.97×10^3	μm/min
Growth exponent	g	1.32	–
Nucleation coefficient	k_b	3.47×10^7	$1/(\mathrm{cm^3 min})$
Nucleation exponent	b	1.78	–
Volume shape factor	k_v	1×10^{-12}	$\mathrm{cm^3/\mu m^3}$
Density of crystals	ρ_c	2.11	$\mathrm{g/cm^3}$
Saturation parameters	A_0	0.1286	g_{KNO_3}/g_{H_2O}
	A_1	5.88×10^{-3}	$g_{KNO_3}/(g_{H_2O}\,^{\circ}\mathrm{C})$
	A_2	1.721×10^{-4}	$g_{KNO_3}/(g_{H_2O}\,^{\circ}\mathrm{C}^2)$
Conversion factor	h	1.246	$\mathrm{cm^3}/g_{H_2O}$
Volume of slurry	V	2056	$\mathrm{cm^3}$

Table 1. Parameter values (Miller and Rawlings 1994).

$$\frac{m_n}{m_s} = \frac{\rho_c k_v V \int_0^{\Delta L_{\text{end}}} L^3 f_n(L, t_{\text{end}})\,\mathrm{d}L}{\rho_c k_v V \int_0^{\Delta L_{\text{end}}} L^3 f_s(L, t_{\text{end}})\,\mathrm{d}L}$$
$$= \frac{V \int_0^{\Delta L_{\text{end}}} L^3 f_n(L, t_{\text{end}})\,\mathrm{d}L}{N_{\text{seed}}(L_{\text{seed}} + \Delta L_{\text{end}})^3} \quad (33)$$

The batch time

$$t_{\text{end}} = \int_0^{\tau_{\text{end}}} \frac{1}{G(\mu_3(\tau), T(\tau))}\,\mathrm{d}\tau \quad (34)$$

is restricted to lie between 50 and 80 min. The yield, i.e. the mass of crystals at the end of the batch

$$m_{\text{end}} = m_n + m_s \quad (35)$$

has to be at least 100 g. The crystallizer temperature $T(t)$ is not allowed to be smaller than 28°C over the whole batch run. The final CSD of nucleated crystals $f_{n,\text{end}}$ is parameterized via third-order splines with spline breaks at 0, 200, 380, 500, 600, 680, 750, 810, 860 μm and ΔL_{end}. The optimization parameters are the 10 function values f_i at the spline breaks and the maximum size $\Delta L_{\text{end}} = \tau_{\text{end}}$. Hence, the following optimization problem has to be solved

$$\min_{f_i, \tau_{\text{end}}} \quad \frac{m_n}{m_s}$$

subject to
$$50\,\text{min} \le t_{\text{end}} \le 80\,\text{min}$$
$$m_{\text{end}} \ge 100\,\text{g}$$
$$T(\tau) \in \mathbb{R} \quad \text{and} \quad T(\tau) \ge 28^\circ\text{C}, \forall\tau$$

This is a non-linear semi-infinite constrained optimization problem, which can be solved, for example, using Matlab. Note that it does not involve any differential equations. The objective function m_n/m_s, the yield m_{end} and the temperature profile $T(\tau)$ can be determined symbolically as functions of the optimization parameters. Only the duration of the batch t_{end} has to be computed numerically by evaluation of the integral (34). The starting values for the optimization parameters are chosen according to the final distribution obtained by linear cooling from 32°C to 28°C.

In figures 4–6 the temperature profiles, final CSDs and supersaturation trajectories are shown for linear cooling, which was used as the starting point of the optimization and for optimized cooling. The cost (33) was reduced from 12.4 for linear cooling to 9.5 for optimal cooling. The qualitative shape of the temperature trajectory matches the results obtained in Miller and Rawlings (1994) by dynamic optimization. The temperature is kept relatively high for the most part of the batch and drops sharply towards the end. This results in low supersaturation over 60 min, thus favouring growth over nucleation. Towards the end of the batch supersaturation rises sharply which results in a rapid growth of

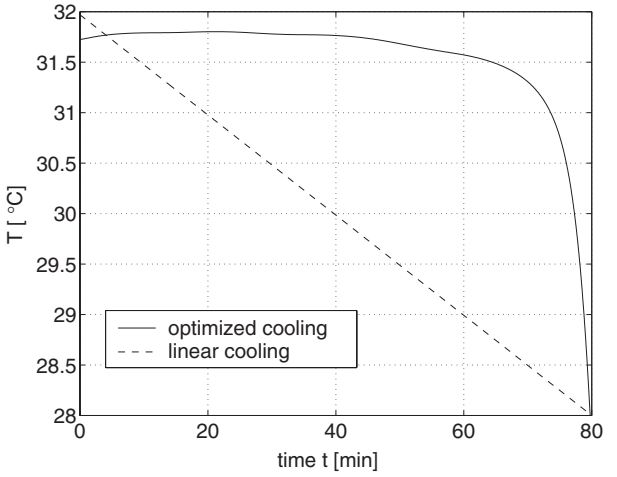

Figure 4. Temperature trajectories: optimized (solid), linear (dashed).

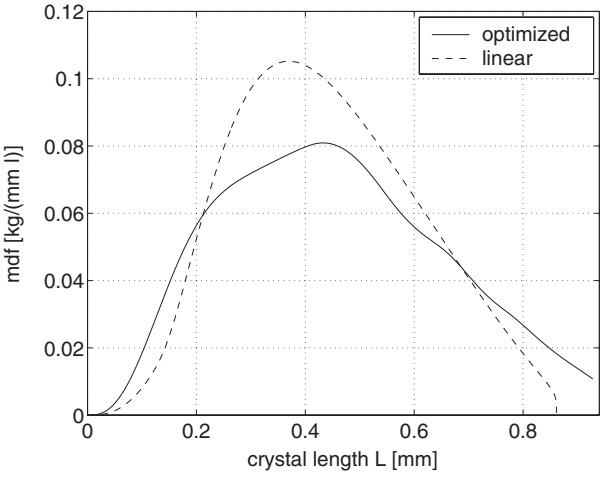

Figure 5. Mass based CSDs (crystals produced by nucleation) obtained by optimized cooling (solid) and linear cooling (dashed).

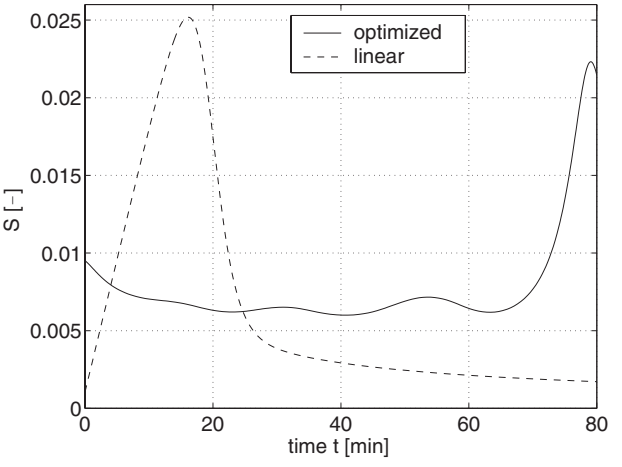

Figure 6. Relative supersaturation corresponding to optimized cooling (solid) and linear cooling (dashed).

existing crystals but also in a burst of nuclei. However, as these nuclei do not have time to grow towards considerable sizes they do not contribute much to the mass of nucleated crystals, which is in the denominator of the cost function (33). Conversely, linear cooling leads to a peak in supersaturation and therefore the production of a large amount of nuclei at an early instant of time. Hence the nuclei have time to grow, which leads to a large mass of nucleated crystals at the end of the batch.

6. Conclusion

This article establishes the fact that moment models for batch crystallization, which are commonly used as a basis for dynamic optimization of these processes, are orbitally flat. The state dependent time scaling function used to render the system flat is physically meaningful. It represents the growth rate of crystals. This leads to a new notion of 'time' which is very natural for the crystallization process: the increase in length of crystals.

The flatness property of the model is exploited for feedforward control design. A procedure is presented to check whether a desired product CSD is achievable and, if so, to determine the corresponding control signal (temperature trajectory) producing this specific CSD. This is a problem that so far had been unsolved in batch crystallization.

Finally, in § 5, it is demonstrated how flatness can be used to facilitate dynamic optimization of batch crystallizer operation. The dynamic optimization problem can be reformulated in such a way that it does not involve any differential equations. Hence the problem is reduced to a parameter optimization problem. As a case study, a particular dynamic optimization problem for the crystallization of KNO_3 is investigated.

Future work will focus on the extension of the methods presented in this contribution to a larger class of models. In particular, the case where crystal growth rate is a function of crystal size is of primary interest.

Furthermore, there are other possibilities to influence the product CSD apart from the temperature profile, which was optimized in this contribution. In particular, the amount and size distribution of seed crystals heavily affects the achievable final CSD. Dynamic optimization has been used in Chung *et al.* (1999) to optimize the seed CSD. This additional degree of freedom can be included in the optimization procedure presented in § 5. As shown in (30), the trajectory of the flat output can be determined by integrating the final CSD four times. The integration constants are determined by the initial condition, i.e. the seed size distribution, which was assumed to be known in advance. If the seed distribution is used as an additional optimization variable, then these constants are free to be varied (within certain bounds). Therefore, it is straightforward to combine optimization of temperature and seed distribution within the framework of flatness based optimization to achieve optimal product quality.

In order to make the process more robust with respect to uncertainties it is desirable to incorporate feedback rather than using pure feedforward control. Since flat systems are linearizable by feedback it is relatively easy to design non-linear feedback tracking controllers for such systems. Therefore, based on the time-scaled moment model, it is possible to design feedback controllers which ensure asymptotic tracking of trajectories of the moments. Such controllers make the tracking error converge to zero exponentially in scaled time τ.

References

Chung, S., Ma, D., and Braatz, R., 1999, Optimal seeding in batch crystallization. *Canadian Journal of Chemical Engineering*, **77**, 590–596.

Fliess, M., Lévine, J., Martin, P., and Rouchon, P., 1992, On differentially flat nonlinear systems. In *Nonlinear Control Systems Design* (Oxford: Pergamon Press), pp. 408–412.

Fliess, M., Lévine, J., Martin, P., and Rouchon, P., 1995 a, Design of trajectory stabilizing feedback for driftless flat systems. *Proceedings of the 3rd European Control Conference ECC'95*, Rome, Italy, pp. 1882–1887.

Fliess, M., Lévine, J., Martin, P., and Rouchon, P., 1995 b, Flatness and defect of nonlinear systems: Introductory theory and examples. *International Journal of Control*, **61**, 1327–1361.

Fliess, M., Lévine, J., Martin, P., and Rouchon, P., 1999, A Lie–Bäcklund approach to equivalence and flatness of nonlinear systems. *IEEE Transactions on Automatic Control*, **44**, 922–937.

Guay, M., 1999, An algorithm for orbital feedback linearization of single-input control affine systems. *Systems Control Letters*, **38**, 271–281.

Guay, M., Kansal, S., and Forbes, J., 2001, Trajectory optimization for flat dynamic systems. *Industrial and Engineering Chemistry Research*, **40**, 2089–2102.

Jones, A., 1974, Optimal operation of a batch cooling crystallizer. *Chemical Engineering Science*, **29**, 1075–1087.

Jones, A., and Mullin, J., 1974, Programmed cooling crystallization of potassium sulphate solutions. *Chemical Engineering Science*, **29**, 105–118.

Lang, Y., Cervantes, A., and Biegler, L., 1999, Dynamic optimization of a batch cooling crystallization process. *Industrial and Engineering Chemistry Research*, **38**, 1469–1477.

Miller, S., and Rawlings, J., 1994, Model identification and control strategies for batch cooling crystallizers. *AIChE Journal*, **40**, 1312–1327.

Ramkrishna, D., 2000, *Population Balances: Theory and Applications to Particulate Systems in Engineering* (New York: Academic Press).

Randolph, A., and Larson, M., 1988, *Theory of Particulate Processes* (San Diego: Academic Press).

Rawlings, J., Miller, S., and Witkowski, W., 1993, Model identification and control of solution crystallization processes: A review. *Industrial and Engineering Chemistry Research*, **32**, 1275–1296.

Respondek, W., 1998, Orbital feedback linearization of single-input nonlinear control systems. *Proceedings of*

IFAC NOLCOS'98, Enschede, The Netherlands, pp. 499–504.

ROTHFUß, R., RUDOLPH, J., and ZEITA, M., 1996, Flatness based control of a nonlinear chemical reactor model. *Automatica*, **32**, 1433–1439.

ROUCHON, P., FLIESS, M., LÉVINE, J., and MARTIN, P., 1993, Flatness and motion planning: the car with *n* trailers. *Proceedings of the 2nd European Control Conference ECC'93*, Groningen, The Netherlands, pp. 1518–1522.

RUDOPH, J., 2000, Boundary control of heat exchangers with spatially distributed parameters: a flatness-based approach. *Automatisierungstechnik*, **48**, 399–402.

RUDOLPH, J., and MOUNIER, H., 2001, Trajectory tracking for pi-flat nonlinear delay systems with a motor example. In A. Isidori, F. L.-L. F. and W. Respondek (Eds) *Nonlinear Control in the Year 2000*, Vol. 2 (London: Springer-Verlag), pp. 339–351.

XIE, W., ROHANI, S., and PHOENIX, A., 2001, Dynamic modeling and operation of a seeded batch cooling crystallizer. *Chemical Engineering Communications*, **187**, 229–249.

ZHANG, G., and ROHANI, S., 2003, On-line optimal control of a seeded batch crystallizer. *Chemical Engineering Science*, **58**(9), 1887–1896.